

The agreement in trend and magnitude demonstrates that the major part of the error is plane orientation. The two maxima near periapse on the  $0.5^\circ$  curve (the curves span exactly one orbit; similar fluctuations occurring on the other three curves are masked by the symbols) occur because, for the orbital geometry investigated, the term  $\sin V$  in the expression  $\theta \nu \sin V$  has a sharp minimum near periapse while the velocity  $\nu$  has a flat maximum.

The strong dependence of the standard deviations on the length of the tracking interval  $T$  results from two strong opposing effects. First, as  $T$  increases, the knowledge of  $i$  improves, because additional data are being taken and the Earth is moving relative to the orbital plane. The Doppler

data most sensitive to orbital plane perturbations are those near periapse. The opposing factor is the perturbation in the Doppler data due to gravity field uncertainties. Because the effect of the gravity coefficients drops off rapidly with radius from the planet, the effects of the nonspherical components of the gravity field are highly concentrated at periapse, and a small variation in the gravity field can produce the same order effect on the Doppler data as a rather large variation in  $i$ . The optimal interval appears to be slightly less than one orbit, starting just after periapse and ending just prior to the next periapse. Utilization of this tracking interval yields uncertainties within the design capability of the current Viking mission.

## Orbit and Position Determination for Mars Orbiters and Landers

R. H. TOLSON,\* W. THOMAS BLACKSHEAR,\* AND SARA G. ANDERSON\*  
NASA Langley Research Center, Hampton, Va.

**Statistical estimates of the state of a spacecraft in orbit about Mars and of the location of a lander on the surface of Mars are generated assuming Earth-based tracking of both spacecraft. The statistics are presented parametrically for a range of orbital geometries, lander locations, and tracking schedules. The satellite geometries are highly eccentric, synchronous orbits consistent with Viking-type mission requirements. The total covariance matrix for the orbiter and lander states includes the effects of model uncertainties in the Martian gravity field, the ephemeris of Mars, and station locations. Eigenvector and eigenvalue analyses relate the tracking geometry to the orientation of the orbiter state error ellipses. The effects of mapping covariances forward in time are also presented.**

**T**HE Viking-type missions are designed to land two spacecraft on the surface of Mars and also to have two spacecraft in orbit about Mars. The orbiters will support the landers through reconnaissance of the landing area and will also act as relay stations for telemetry to the Earth if the direct link from the lander to the Earth is inoperable. There are various mission phases which require accurate knowledge of the location of the lander and the dynamical state of the orbiter. The purpose of this paper is to present some results of preliminary studies of the accuracy of determining the lander and orbiter states. Further, problem areas are indicated for which additional studies are required.

The results presented herein are restricted to the types of tracking data and orbital geometries expected during the Viking mission. The two types of tracking data that may be available are Earth-based range (light travel time) and range rate (Doppler) to all spacecraft. The Earth-based range rate data are assumed to be unbiased and to have a random noise of 1 mm/sec. Excluding periods of occultation, this type of data will be available essentially continuously from the orbiters; however, a more limited availability is expected from the landers due to power considerations. Although this paper has assumed a 1974 encounter date, the results should generally apply to the 1976 encounter as well.

The Earth-based range data appear to have limited operational or real-time utility after the spacecraft reaches Mars and, consequently, no consideration is given to range data in the analyses presented here. The reason for its ineffectiveness is the large uncertainties in the Martian ephemeris relative to

the Earth. The anticipated radial ephemeris uncertainty during the mid-1970 time period is 5 km which is very large compared to the noise on the range data of 15 m. Simulations have shown that even if the ephemeris errors were negligible, the range data contribute little knowledge to the orbit determination as long as Doppler data are also available. However, as will be shown later, Doppler data are not very effective for completely determining the lander position, and preliminary studies indicate that range data could be very useful in completing the definition of the lander location if the ephemeris errors were somewhat smaller. It does not appear feasible to simultaneously determine the lander location and the Martian ephemeris because of the high correlation between these parameters for the short data arcs available during the early phases of the real-time mission. However, over longer data arcs the ephemeris and lander location effects become separable and the range data will then be a very effective data type.

The statistical model is based on the assumption that the estimator utilizes a weighted least-squares (WLS) process where the data are unbiased and uncorrelated and the weighting matrix is the inverse of the data covariance. The estimator does not account for known model errors and, consequently, is not optimal but is characteristic of processes currently in use for orbit determination. The equations are linearized and in the following discussion only the linearized equations are analyzed. Lower-case letters represent vectors, upper-case letters are matrices, and all dimensions are assumed consistent. Let  $x$  be the state vector at epoch to be estimated,  $y$  the observable,  $p$  an unknown vector which shall include dynamic and observation model uncertainties, and  $e$  the noise on the data. To generate statistics on the estimator  $\hat{x}$  of  $x$  it is assumed that  $p$  is a random vector with mean zero [ $E(p) = 0$ ] and covariance  $\text{cov}(p) = P_p$ . Further, it is as-

Presented as Paper 70-160 at the AIAA 8th Aerospace Sciences Meeting, New York, January 19-21, 1970; submitted March 10, 1970; revision received June 15, 1970.

\* Aerospace Technologist.

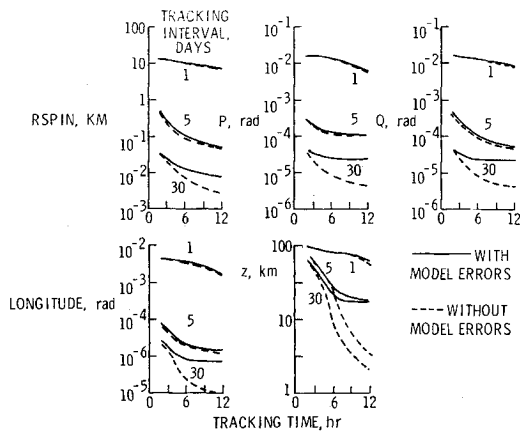


Fig. 1a Lander position standard deviations. Tracking starts on Feb. 14, 1974.

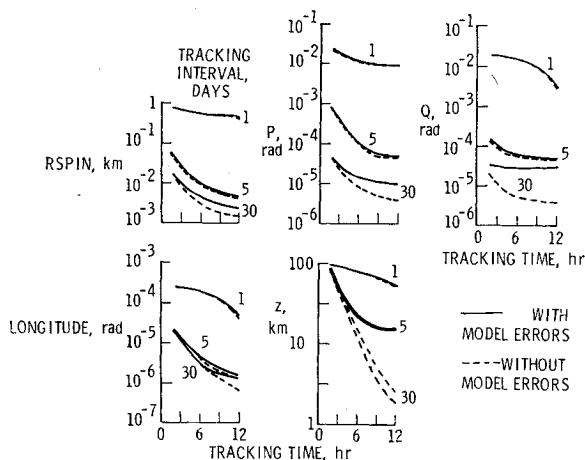


Fig. 1b Lander position standard deviations. Tracking starts on April 15, 1974.

sumed that  $E(e) = 0$ ,  $\text{cov}(e) = P_e$ , and  $E(pe^T) = 0$ , where superscript  $T$  indicates the transposed array.

The equation relating the observations to the parameters is

$$y = Ax + Cp + e \quad (1)$$

The WLS estimator

$$\hat{x} = (A^T P_e^{-1} A)^{-1} A^T P_e^{-1} y \quad (2)$$

is one of the unbiased estimators of  $x$  since  $E(\hat{x}) = x$ . The covariance of  $\hat{x}$ ,

$$P_{\hat{x}} = E[(\hat{x} - x)(\hat{x} - x)^T]$$

is not minimal but will reduce to

$$P_{\hat{x}} = (A^T P_e^{-1} A)^{-1} + (A^T P_e^{-1} A)^{-1} A^T P_e^{-1} C P_p^{-1} C^T P_e^{-1} A (A^T P_e^{-1} A)^{-1} \quad (3)$$

with the use of Eqs. (1) and (2) and the assumptions above. A priori statistics on  $\hat{x}$  can be combined with the above in the usual statistical manner for independent variables. Variants of Eq. (3) that accounts for a priori statistics on  $\hat{x}$  and that map the statistics at epoch to other times are used in the rest of the paper to generate all statistics.

Table 1 gives the a priori statistics assumed for each term in both the  $x$  and  $p$  arrays. The initial standard deviations in the orbiter rectangular state components are set at arbitrary, large values. The lander position is most naturally represented by cylindrical coordinates and the a priori standard deviations are taken to be consistent with expected landing

dispersions and surface elevation uncertainties. To completely define the lander location in inertial space three additional parameters are required, and these are chosen to be the Martian pole location and rotational period of Mars. The Earth-based tracking station locations are also specified in a cylindrical system and the standard deviations in Table 1 are consistent with the expected uncertainties during the time period of interest. The six components of the Martian ephemeris relative to the Sun are assumed to be spherically distributed about the mean with the indicated component standard deviations. The current uncertainty in the gravitational constant of Mars is shown in the table. This value might be reduced as planetary mission data are processed. The table also shows the uncertainties assumed for the gravity coefficients of the Martian gravity field. The values used here are based on an analysis in Ref. 1 that can be used to predict what values of gravity coefficients can be expected for planets other than the Earth. Nonspherical gravity terms through degree and order 4 are included as errors in the orbit determination process.

### Lander Position Location

The methods to be used for determining the location of the landed spacecraft on Mars are analogous to the methods used to determine the location of tracking stations on the Earth. In fact, one of the most effective and often-used methods for determining station longitude and distance off the Earth spin axis ( $r$  spin) is to utilize horizon to horizon Doppler tracking of a known, nearly fixed point in deep space. Such procedures have led to determining the above parameters to an accuracy of a few meters. However, the procedure is not very effective for determining the position ( $Z$ ) of the tracking station parallel to the spin axis. From the aerocentric viewpoint, the landed spacecraft can be thought of as tracking a known, nearly fixed point in deep space, namely, the Earth tracking station. Horizon-to-horizon tracking is possible because of the relatively high rotational rate of Mars. In fact, due to the

Table 1 A priori standard deviations

Parameter	Standard deviation
Orbiter position	1000 km
Orbiter velocity	1 km/sec
Lander longitude	1 deg
Lander distance off the spin axis	40 km
Lander Z component	100 km
Martian polar locations	1 deg
Martian rotational period	$5 \times 10^{-7}$ hr
Station distance off the spin axis	0.0015 km
Tracking station Z component	0.025 km
Tracking station longitude	$4.7 \times 10^{-7}$ rad
Ephemeris position	5 km
Ephemeris velocity	$5 \times 10^{-7}$ km/sec
Astronomical unit	2 km
Martian GM	$1.43 \text{ km}^3/\text{sec}^2$
Martian gravity field coefficients	
$n$	$m$
2	0
2	1
2	2
3	0
3	1
3	2
3	3
4	0
4	1
4	2
4	3
4	4
	$3.9 \times 10^{-5}$
	2.2
	1.1
	2.0
	0.83
	0.26
	0.11
	1.3
	0.41
	0.097
	0.026
	0.009

similarity between the terrestrial and Martian rotation rates and sizes, it will not be surprising if the same order accuracies result for determining the lander longitude and  $r$  spin as are obtained for the corresponding Earth tracking stations' parameters.

An additional complication arises in determining the lander location on Mars, due to the uncertainty in the direction that the Martian pole points in space. This error could be as large as  $1^\circ$ , which is equivalent to about 60 km on the surface. An error in pole location will cause the apparent latitude and  $r$  spin to vary as the planet rotates. Because of the possible large errors in position resulting from this cause, it will be necessary to determine the pole location from the tracking data. The model used for this study assumes that the true pole differs from the assumed pole by a small angle, which is represented by two rotations  $P$  and  $Q$ . The pole displacement in aerocentric declination is denoted by  $P$ , and  $-Q$  is the displacement in aerocentric right ascension. The final variable, of the required six, necessary to define the lander position uniquely is the rotational period of Mars. This parameter is known so accurately that its uncertainty need not be significantly reduced via the tracking data.

A parametric study was performed using various length tracking periods per day, total tracking spans, lander locations, and initial epochs. The results were not significantly affected by the lander latitude over the range of interest from  $30^\circ$  S to  $30^\circ$  N. Typical results of these studies are present in Fig. 1 for a lander at zero latitude. Figs. 1a and 1b are for the cases where the tracking interval starts on February 14 and April 15, 1974, respectively. The figure presents the variations in the lander position and pole location standard deviations for tracking spans of 1, 5, and 30 days, and for a range of tracking intervals per Martian day from 2 to 12 hr. The 30-day case actually has a 5-day tracking interval at the beginning and end of the 30 days and 20 days in the middle during which no data are taken. The daily tracking intervals are centered about the same time that the Earth crosses the lander meridian. The solid curve is generated using Eq. (3) with the a priori uncertainty for the lander parameters and the appropriate model errors. The dashed curves were generated using just the first term in Eq. (3) and corresponds to the statistics which would result if there were no model errors.

The first point to be noted from the figure is that a single day of tracking produces little information about  $P$ ,  $Q$ , and  $Z$ . Yet substantial improvements in  $r$  spin and longitude are noted even for this short tracking interval. The 5- and 30-day tracking intervals result in substantial reductions in all standard deviations. The approximate order of magnitude reduction in the  $r$  spin and longitude standard deviations from February 14 to April 15 is due to the change in the aerocentric declination of the Earth during this time. In February, the declination is  $-14^\circ$  and in April the Earth is crossing the Martian equator heading north. When the Earth is on the equator, the uncertainties in longitude and  $r$  spin are not coupled with the pole location uncertainties and the other uncertainties in the model have less influence at this time.

The model errors that contribute the most to the final covariance are the ephemeris errors. If this error source could be eliminated, the accuracies indicated by the dashed lines could nearly be achieved. This would yield a determination of longitude,  $r$  spin,  $P$ , and  $Q$  in the 10-m range, which is consistent with the analogous results obtained for Earth-tracking stations. It appears that additional length of the data arcs would result in further reductions for some of the variables while others have reached the asymptotic limit. In order to effect further reductions in these latter variables, the model errors would have to be reduced by some means. The  $Z$  component remains the largest contributor to the total error in position. The limiting value is a strong function of the daily tracking interval varying from about 90 km to 20 km as the daily tracking interval varies from 2 hr to half a Martian day. A more

extensive analysis<sup>2</sup> has shown that dividing the 2-hr tracking interval into three equal periods near the times of Earth rise, Earth meridian crossing, and Earth set can yield accuracies similar to those obtained for the longer tracking intervals. However, if a more precise lander location is desired, means must be found to either eliminate the ephemeris errors or obtain a new observation source.

A procedure to eliminate the radial component of the ephemeris error and thus make ranging a more useful data type for determining lander position has been tested in a limited manner and the results have been very encouraging, although further study is required to prove the technique. The technique is based on using nearly simultaneous Doppler and ranging data to both an orbiter and a lander. First orbiter Doppler data, which are not very sensitive to the ephemeris errors, are processed to estimate the orbiter state. The resulting orbital plane passes very near the center of mass of Mars; consequently, when the orbiter range data are processed, using this orbital plane, the radial ephemeris errors appear as a nearly constant range bias. The ephemeris is then updated by the amount of the range bias for the processing of the lander range and Doppler data.

### Satellite Orbit Determination

The geometric characteristics of the nominal orbits are rather restricted except for the inclination. The period, which must be nearly synchronous with the rotation period of Mars for reconnaissance purposes, is 24.6 hr and yields a semi-major axis of about 20,400 km. The nominal periape altitude is determined from energy, telecommunications, and reconnaissance considerations to be 1400 km. The combination of these two values gives a very elliptical orbit with an ec-

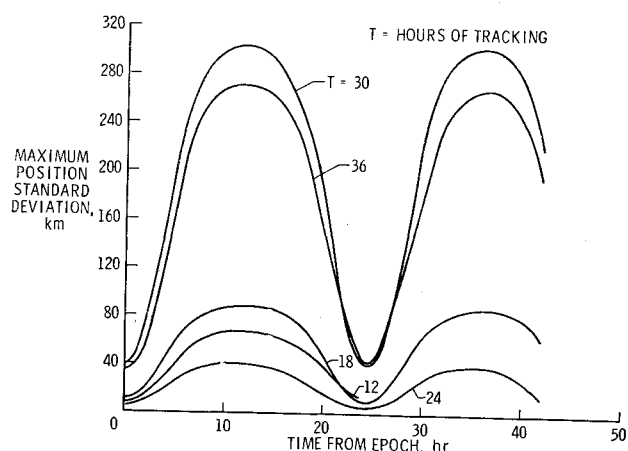


Fig. 2a Position standard deviation for epoch at periapse and orbital inclination of  $30^\circ$ .

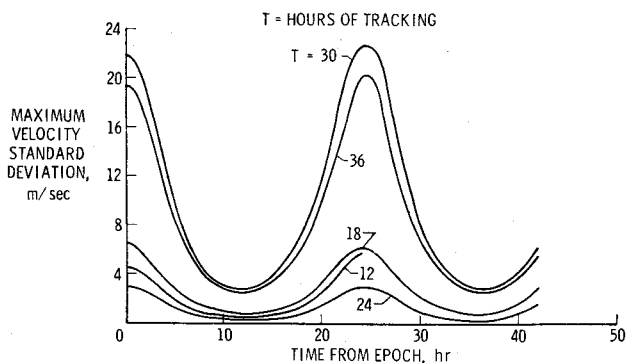
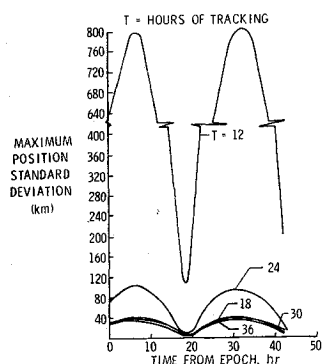
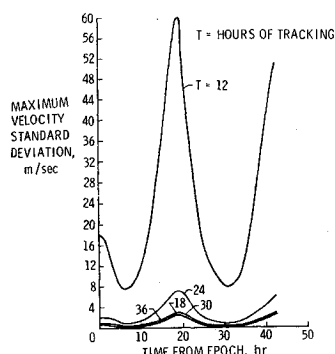


Fig. 2b Velocity standard deviation for epoch at periapse and orbital inclination of  $30^\circ$ .



**Fig. 3a** Position standard deviation for epoch at 6 hr after periapse and orbital inclination of  $30^\circ$ .



**Fig. 3b** Velocity standard deviation for epoch at 6 hr after periapse and orbital inclination of  $30^\circ$ .

centricity of 0.766. Because the orbit is established from an interplanetary approach trajectory in a nearly minimal energy fashion, the major flexibility remaining for mission design is a rotation of the orbit about the approach direction. The inclination, which will be defined by the latitude of the landing site, can vary from about  $-20^\circ$  to  $60^\circ$ . The Earth moves relative to the orbit plane because of the nodal regression due to oblateness and the relative motion of the two planets. However, this apparent motion is only about  $0.6^\circ$  per day or per orbit.

This comparatively slow motion of the Earth relative to the orbital plane introduces a serious orbit determination problem. For it is well known that if there were no relative motion it would be impossible to completely determine all of the orbital elements from Doppler observations. In particular, with either Doppler or range data, the orientation of the orbit about the line of sight from the Earth to Mars is indeterminate. Orbit determination for lunar satellites<sup>3</sup> suffers from a similar geometric weakness that can be partially alleviated by using simultaneous data from Earth-based stations having a large dispersion in latitude and longitude. The selenocentric parallax of such tracking stations can be four times the angular motion of the Earth in one orbit and, consequently, this technique is a powerful means of eliminating the indeterminacy. However, for Martian satellites the parallax introduced by this means is only 10 sec of arc and is very small compared to the angular motion of the Earth during one orbit. Therefore, this technique will not improve the situation and it can be anticipated that the major uncertainty for Martian satellite orbit determination will be in the orientation of the orbital plane about the line of sight. Earlier analyses, for example Ref. 4, have arrived at the same conclusion and have demonstrated the quantitative effects under the assumption that the only errors were data noise. This assumption leads to the same unrealistically small estimates of Martian satellite state uncertainties as were obtained in Ref. 3 for lunar satellites. A more conservative and realistic approach is to perform the error analysis using Eq. (3), while including in the  $p$  array all unestimated observational and dynamical uncertainties.

In order to better understand the problems associated with orbit determination of a highly eccentric Martian satellite, a

parametric study was performed for the typical Viking geometries discussed previously and for two inclinations of  $30^\circ$  and  $60^\circ$ . Tracking intervals of 12, 18, 24, 30, and 36 hr were analyzed, and for each tracking interval the epoch time was taken to be at four points in the orbit corresponding to periapse, periapse plus 6 hr, apoapse, and apoapse plus 6 hr. The statistics at epoch for a weighted least-squares process were generated using Eq. (3), assuming Doppler measurements at 10-min intervals with a random noise of 0.001 m/s, and using all appropriate a priori standard deviations from Table 1. The epoch statistics were mapped to other points in the orbit to investigate the variation with position in orbit and mapping time.

The results of this parametric analysis are presented in Figs. 2-5, in the form of the maximum position and velocity eigenvalues as a function of the time from epoch for the five values of the tracking interval length. For example, consider the curve in Fig. 2a corresponding to 24 hr of tracking. The data span the interval starting at time from epoch (periapse) equal zero to time from epoch equal 24 hr (0.6 hr prior to periapse). The statistics at epoch are then mapped through the first orbit and most of the second orbit. The position and velocity eigenvalues were obtained by diagonalizing the respective  $3 \times 3$  covariance submatrices.

The first point to be noted from all these figures is the generally periodic nature of the results with only a small amount of secular growth. This characteristic tends to confirm the anticipated result that the major uncertainty is due to an uncertainty in the orientation of the orbital plane. Further confirmation is based on a calculation of the angle between the position (velocity) eigenvector corresponding to the maximum position (velocity) uncertainty eigenvalue and the normal to the plane defined by the position (velocity) vector and the Mars-Earth vector. If the total uncertainty were due to an infinitesimal rotation about the line of sight, these two angles would be theoretically zero. The observed variation, over nearly all of the results present in the figures, was less than  $2^\circ$ . In the cases where the angles are small, the ratio of the maximum to the intermediate standard deviation is usually greater than 25. Thus, these cases are characterized by a unidirectional, nearly

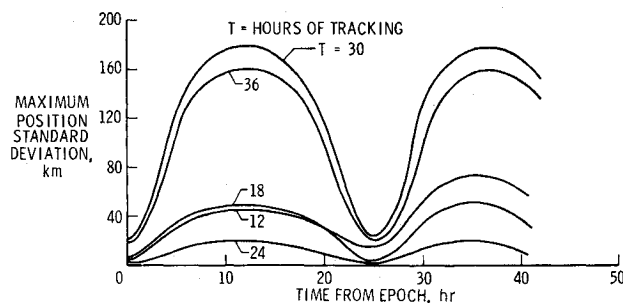


**Fig. 4a** Position standard deviation for epoch at periapse and orbital inclination of  $60^\circ$ .

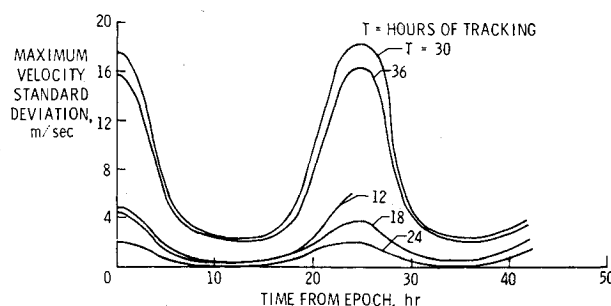


**Fig. 4b** Velocity standard deviation for epoch at periapse and orbital inclination of  $60^\circ$ .

degenerate error ellipsoid. For a small rigid rotation  $\theta$  of the orbital plane about the Earth-Mars line, the expected change in position is  $\theta r \sin R$ , where  $r$  is the radial distance of the satellite from Mars and  $R$  is the angle between the Earth-Mars line and the position vector. A similar expression,  $\theta v \sin V$ , holds for the corresponding velocity change, where  $v$  is the satellite velocity relative to Mars and  $V$  is the angle between the Earth-Mars line and the velocity vector. For the orbit geometries presented herein, these expressions can be used to determine the orbit plane uncertainty corresponding to the indicated position and velocity uncertainties. The approximate relation is:  $1^\circ$  of plane rotation about the line of sight produces approximately 630 km of position displacement at apoapse. For example, from Fig. 3a it is seen that the plane orientation has an uncertainty of over a degree when only 12 hr of data are taken. This is not surprising, since the data span true anomalies from about  $160^\circ$  to  $200^\circ$ . During the time that these data are taken, the satellite is moving at a low velocity and the Doppler data are relatively insensitive to changes in the orbital elements. An actual comparison between the maximum velocity and position standard deviations due to orbital plane rotations is shown in Fig. 6. The symbols correspond to the points generated in the error analysis that were used to plot part of Fig. 2. The solid curves correspond to the deviations calculated, using the above expressions, with plane rotations ( $\theta$ ) of  $0.5^\circ$  and  $0.14^\circ$ . The agreement in trend and magnitude demonstrates that the major part of the error is plane orientation. One unexpected result is the illustrated double maximum in the vicinity of periapse on the  $0.5^\circ$  curve (the curves span exactly one orbit and are essentially periodic). Similar fluctuations occurring on the other three solid curves are masked by the symbols. This effect is due to the fact that for the orbital geometry investigated the term  $\sin V$  in the expression  $\theta v \sin V$  has a sharp minimum near periapse while the velocity ( $v$ ) has a flat maximum. The resulting product has the indicated double maximum.

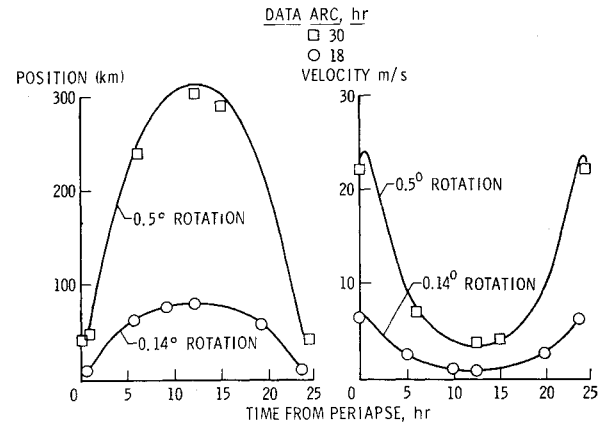


Fig. 6 Comparison of exact errors with displacements due to rigid rotations about Earth-Mars line.

For a fixed orbital orientation and epoch location, the standard deviations are seen to depend very strongly on the length of the tracking interval. This radical fluctuation is produced by two very strong opposing effects. First, as the length of the tracking interval increases, the knowledge of the plane orientation improves because additional data are being taken and the Earth is moving relative to the orbital plane. The position in orbit that produces the Doppler data most sensitive to orbital plane perturbations is in the vicinity of periapse. A sensitivity analysis was performed in which simulated Doppler data were generated for the case represented by Fig. 2. The orbit plane was then rotated  $1^\circ$  about the line of sight at epoch and additional Doppler data were generated, all other factors being equal to the first case. A comparison of the two sets of data showed a difference of about 0.06 m/s at the apoapse following epoch and 0.9 m/s at the next periapse. This variation is plotted in a nondimensional manner in Fig. 7. Thus, if there were no other considerations, the orientation uncertainty could be most effectively reduced by processing data taken near successive periapse passes. These phenomena can be observed by comparing the results for the two 12-hr tracking interval cases with the epoch 6 hours after periapse and at periapse (Figs. 3 and 2). In the latter case, the inclusion of the data near periapse produces a factor of 13 improvement in knowledge of the orbit plane orientation.

The second and opposing factor also has its dominant effect at periapse; namely, the perturbation in the Doppler data due to gravity field uncertainties. Because the effect of the gravity coefficients drops off rapidly with radius from the planet, the effects of the nonspherical components of the gravity field are highly concentrated at periapse. A sensitivity analysis was also performed by varying the second degree zonal harmonic by  $3 \times 10^{-4}$  or 15% of its estimated known value and comparing the Doppler data for the same case as above. Be-

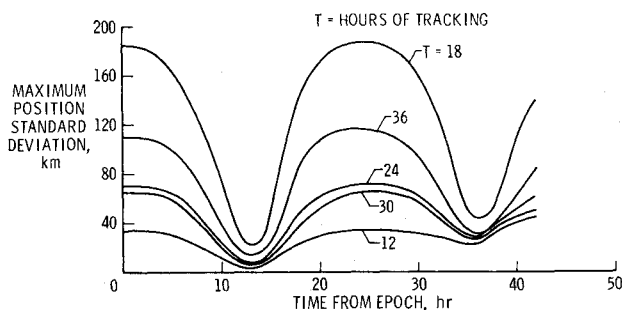


Fig. 5a Position standard deviation for epoch at apoapse and orbital inclination of  $60^\circ$ .

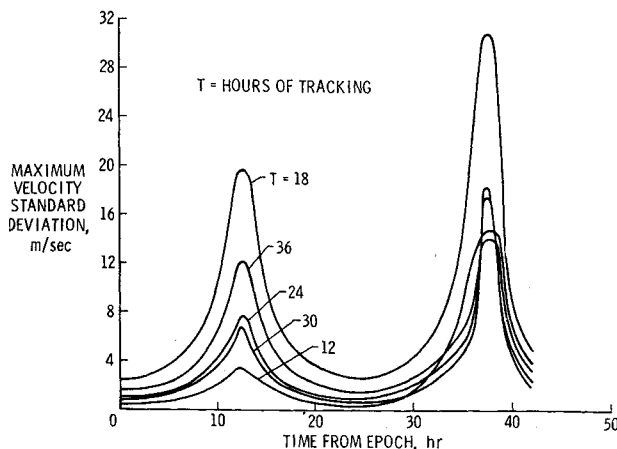


Fig. 5b Velocity standard deviation for epoch at apoapse and orbital inclination of  $60^\circ$ .

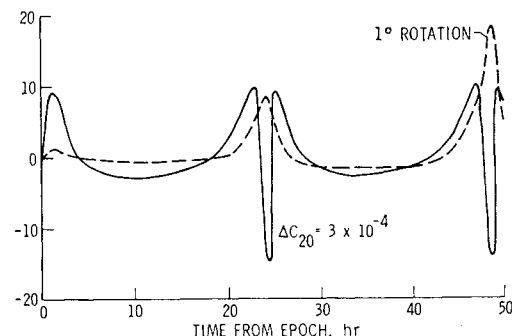


Fig. 7 Sensitivity of Doppler data to orbital plane rotations and planetary oblateness.

fore the comparison was made, the semimajor axis of the orbit was adjusted to remove all secular effects produced by varying the coefficient. The resulting differences are illustrated in Fig. 7. It is seen that a small variation in the gravity field can produce the same order effect on the Doppler data as a rather large plane orientation variation. The signatures are not identical and, consequently, the entire gravity field error is not absorbed by the orientation angle; however, as indicated by the results presented in Figs. 2-5, a substantial portion of the model error is absorbed.

The conclusion to be drawn from this discussion is that in order to obtain the most accurate orbit determination, enough data near periapse must be processed to reduce the orbital plane uncertainty but not enough to allow the gravity field uncertainties to corrupt the solution. The optimal interval appears to be slightly less than one complete orbit, starting just after periapse and ending just prior to the next periapse. The uncertainties resulting from the near optimal tracking interval are well within the design capability of the current mission. However, further effort is required to define the optimal tracking interval and its sensitivity to orbit geometry, tracking data noise, and values of the a priori uncertainties in the gravity coefficients and estimated state variables.

### Concluding Remarks

It has been seen that both the lander position determination and the satellite orbit determination processes have one degree of near indeterminacy. For the landed spacecraft, the displacement along the Martian spin axis is very poorly determined. For tracking intervals up to 30 days and with the anticipated ephemeris errors, the ultimate knowledge will vary between 80 and 15 km as the amount of tracking data per

Martian day varies from 2 to 12 hr. Additional knowledge can be gained by utilizing other information such as measurements made onboard the lander, reconstruction of the entry trajectory, and Earth-based range data filtered with more sophisticated data processing techniques than are simulated herein.

The satellite orbit determination suffers from the lack of sensitivity of the Earth-based tracking data to rotation of the orbital plane about the line of sight. The uncertainties in the satellite state are seen to depend very strongly on the length of the tracking interval and the position of the tracking arc along the orbit. Such strong variations indicate that great care must be exercised in the real-time orbit determination process to remove as many model errors as possible, because small model errors can contribute large biases in the plane orientation. Further analysis is required in the area of optimal tracking intervals and consideration should be given to the use of optimal filters instead of the weighted least-squares process analyzed herein.

### References

- <sup>1</sup> Kaula, W. M., *Theory of Satellite Geodesy*, Blaisdell, Waltham, Mass., 1966.
- <sup>2</sup> Russell, R. K., "Lander Transponder Estimated for Short Data Spans," TM 391-48, Dec. 1969, Jet Propulsion Lab.
- <sup>3</sup> Tolson, R. H. and Compton, H. R., "Accuracy of Determining the State of a Lunar Satellite and the Lunar Gravitational Field," *Journal of Spacecraft and Rockets*, Vol. 4, No. 1, Jan. 1967, pp. 26-33.
- <sup>4</sup> Russell, R. K., *Satellite Orbit Determination Accuracy Study Applicable to Voyager Trajectories*, SPS 37-45, Vol. II, Jet Propulsion Lab.